

## Supplementary information

### **SQUID-on-tip with single-electron spin sensitivity for high-field and ultra-low temperature nanomagnetic imaging**

Y. Anahory<sup>1\*</sup>, H.R. Naren<sup>2</sup>, E.O. Lachman<sup>2</sup>, S. Buhbut Sinai<sup>3</sup>, A. Uri<sup>2</sup>,  
L. Embon<sup>2</sup>, E. Yaakobi<sup>2</sup>, Y. Myasoedov<sup>2</sup>, M.E. Huber<sup>4</sup>, R. Klajn<sup>3</sup> and E. Zeldov<sup>2</sup>

<sup>1</sup>Racah Institute of Physics, The Hebrew University, Jerusalem 91904, Israel

<sup>2</sup>Department of Condensed Matter Physics, Weizmann Institute of Science, Rehovot 7610001, Israel

<sup>3</sup>Department of Organic Chemistry, Weizmann Institute of Science, Rehovot 7610001, Israel

<sup>4</sup>Departments of Physics and Electrical Engineering, University of Colorado Denver, Denver 80217, USA

\*Corresponding author: [yonathan.anahory@mail.huji.ac.il](mailto:yonathan.anahory@mail.huji.ac.il)

## Measurement of I-V characteristics

The measurement circuit, illustrated schematically in Fig. S1, consists of a room temperature voltage source that provides the bias current  $I_B$  through the low temperature bias resistor  $R_B$ , with a typical value of a few k $\Omega$ . The SOT is effectively voltage-biased by the low-resistance shunt resistor  $R_S$ , with a value of a few  $\Omega$ , in presence of a parasitic resistance  $R_p$ . The current through the SOT,  $I_{SOT}$ , was measured using a SQUID series array amplifier (SSAA) as described in Refs.<sup>1,2</sup> and identified in Fig. S1 as A. The SSAA is inductively coupled to the SOT circuit through a superconducting coil  $L_{in}$ . Warm electronics applies a voltage  $V_{FB}$  to maintain a constant flux in the SSAA. In flux-locked loop conditions,  $I_{FB} \propto I_{SOT}$  and  $I_{FB}$  is itself proportional to the voltage drop  $V_{FB}$  on a resistor  $R_{FB}$ , with a typical value of a few k $\Omega$ . Thus,  $V_{FB}$  is a direct readout of  $I_{SOT}$ .

Figure S2a,c,e shows the raw  $I_{SOT}$ - $I_B$  curves of a SOTs at 300 mK for different materials. The  $I_{SOT}$ - $I_B$  curves can be separated into two regions. Below  $I_c$ , a linear region with slope  $R_S/(R_S + R_p)$  represents the state where the SOT is superconducting. For larger values of  $I_B$ , the SOT is in the voltage state and the curve is no longer linear. Knowing the voltage on the shunt resistor  $V_S = R_S(I_B - I_{SOT})$ , and the voltage on the parasitic resistance  $V_p = R_p I_{SOT}$ , we calculate  $V_{SOT} = V_S - V_p$ . From this result, we can then present the  $I_{SOT}$ - $V_{SOT}$  curves (Fig. S2 b,e,f).

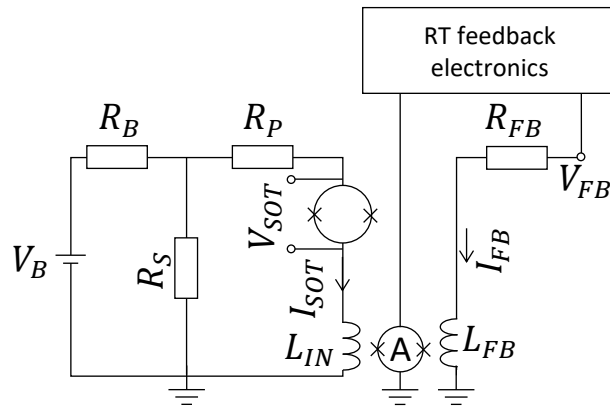


**Figure S1 – Detailed measurement circuit.**  $R_B$  and  $R_{FB}$  are typically a few k $\Omega$ ,  $R_S$  a few ohms, and  $R_p$  ideally below 1 ohm. All of the circuit except for the room-temperature feedback electronics is at 300 mK.

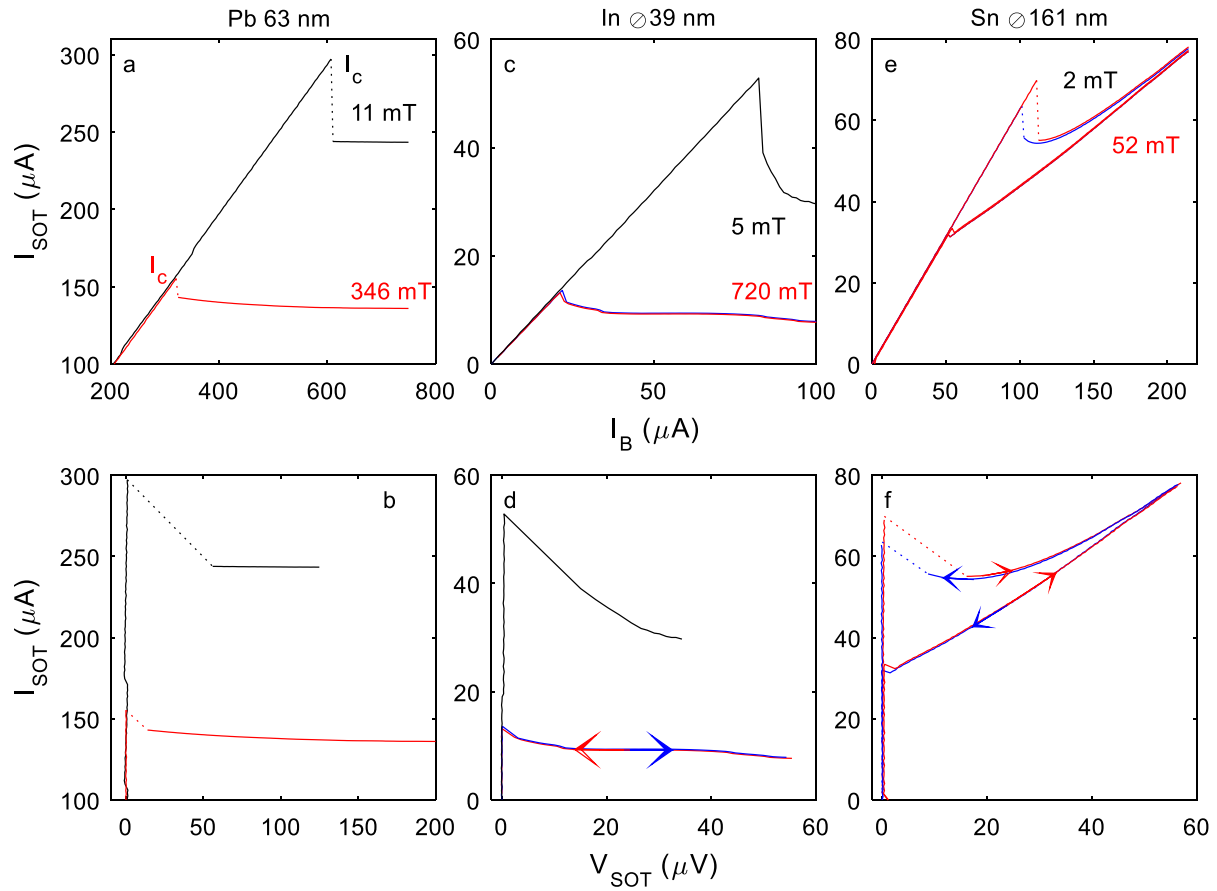


**Figure S2 -  $I$ - $V$  characteristics of SOT devices made of different materials at 300 mK. (a-f)  $I$ - $V$  characteristics of three different SOT devices at two different applied magnetic fields. (a)  $I_{SOT}$ - $I_B$  curve of a hysteretic unshunted Pb SOT with diameter of 63 nm ( $R_B = 2.0$  k $\Omega$ ,  $R_S = 3.0$   $\Omega$ ,  $R_P = 3.1$   $\Omega$ ). (b) The corresponding  $I_{SOT}$ - $V_{SOT}$  characteristics of the Pb device. (c)  $I_{SOT}$ - $I_B$  characteristics of an In SOT of 39 nm diameter with integrated shunt-on-tip ( $R_B = 7.0$  k $\Omega$ ,  $R_S = 3.0$   $\Omega$ ,  $R_P = 1.8$   $\Omega$ ) and its corresponding  $I_{SOT}$ - $V_{SOT}$  characteristics (d). The red (blue) curve shows the measurement upon ramping  $I_B$  up (down). (e)  $I_{SOT}$ - $I_B$  characteristics of a slightly hysteretic shunted Sn SOT with diameter of 162 nm ( $R_B = 7.0$  k $\Omega$ ,  $R_S = 3.0$   $\Omega$ ,  $R_P = 1.8$   $\Omega$ ) with its corresponding  $I_{SOT}$ - $V_{SOT}$  characteristics (f). The inset shows a simplified diagram of the measurement circuit.**

### Additional Fe<sub>3</sub>O<sub>4</sub> nanocube images at zero field

Small particles such as Fe<sub>3</sub>O<sub>4</sub> nanocubes can have defects that might influence the observations in this work. Here we show four other nanocubes that were imaged with the same 150 nm diameter In SOT as in the main text at the same temperature of about 300 mK. These images were also taken after ramping the field to 0.36 T. The out-of-plane field  $B_z(x, y)$  images are shown in Fig. S3 a-c. For each of the images, the magnitude of the magnetic moment,  $m_0$ , as well as its polar,  $\theta$ , and azimuthal,  $\phi$ , angles were derived by performing a numerical fit of the data. Our model comprises a finite size SQUID loop with fitting parameters  $m_0$ ,  $\theta$ ,  $\phi$  and the SOT-to-nanocube distance. The corresponding numerically attained best-fit stray field maps are presented in Figs. S3 d-f. The subtraction of the experimental and the corresponding best-fit image to show the quality of the fit is shown in Figs. S3 g-i. The magnitude and the polar angle are consistent with the finding shown in the main text. We have no evidence of other nanocubes behaving in a significantly different manner.

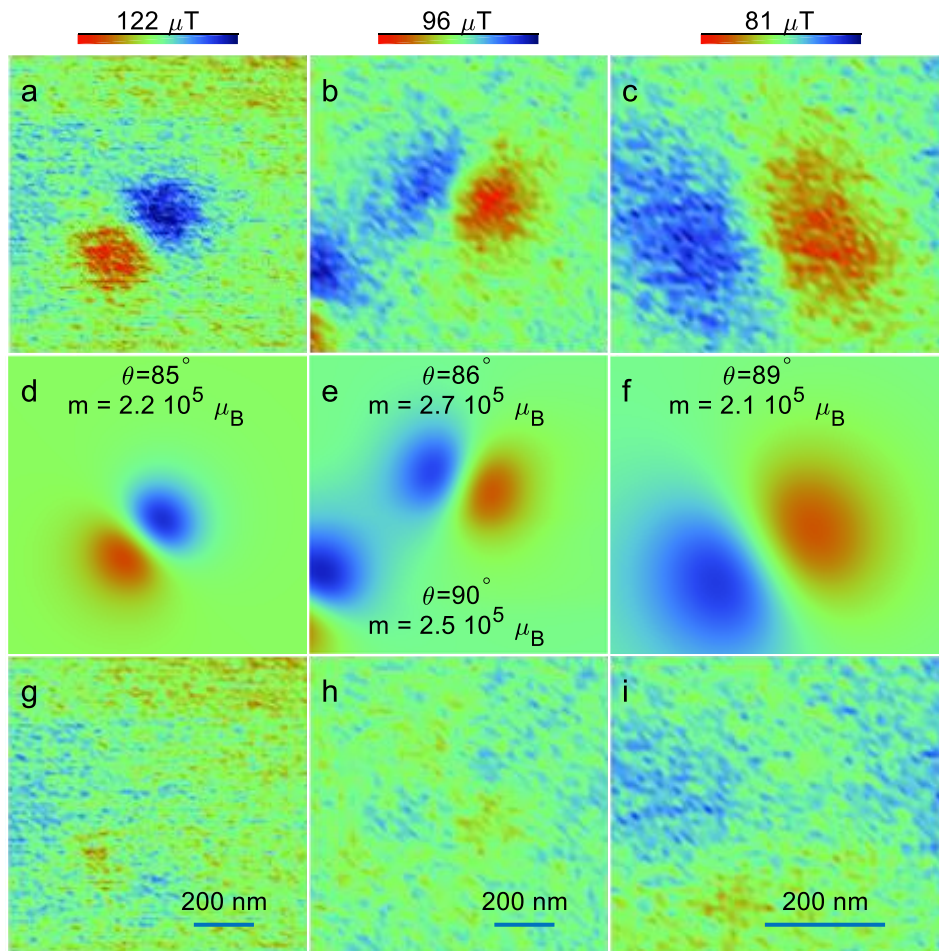


**Figure S3 - Additional images at zero field** – (a-c) Stray field  $B_z(x, y)$  of different Fe<sub>3</sub>O<sub>4</sub> nanocube at  $\mu_0 H_z = 0$  T. (d-e) Corresponding best fit numerically simulated  $B_z(x, y)$  with magnetic moment and polar angle found for each nanocube. The best tip-to-sample distance fit was 141 (d), 171 (e) and 165 nm (f) (g-h) Subtraction of the experimental image and the corresponding fit.

## References

1. A. Finkler, Y. Segev, Y. Myasoedov, M. L. Rappaport, L. Ne'eman, D. Vasyukov, E. Zeldov, M. E. Huber, J. Martin, and A. Yacoby, "Self-aligned nanoscale SQUID on a tip", *Nano Lett.* **10**, 1046 (2010).
2. D. Vasyukov, Y. Anahory, L. Embon, D. Halbertal, J. Cuppens, L. Neeman, A. Finkler, Y. Segev, Y. Myasoedov, M. L. Rappaport, M. E. Huber, and E. Zeldov, "A scanning superconducting quantum interference device with single electron spin sensitivity", *Nat. Nanotechnol.* **8**, 639 (2013).